Non-adiabatic Effects in Electron Momenta

C. Hofmann, A. S. Landsman, C. Cirelli, U. Keller
Physics Department, ETH Zurich, 8093 Zurich, Switzerland
chofmann@phys.ethz.ch

Abstract: In strong-field tunnel ionization of Helium, both adiabatic and fully non-adiabatic theoretical descriptions predict smaller final longitudinal electron momentum distributions than measured experimentally. Semiclassical simulations including an initial longitudinal momentum spread reproduce experimental values.
OCIS codes: (020.2649) Strong field laser physics; (320.7120) Ultrafast phenomena

1. Strong Field Ionization

In many attosecond science methods, tunnel ionization in a strong laser field is the first step. Both adiabatic [1,2] and non-adiabatic [3–5] models are applied to interpret experimental data. Common to all models is the debate on the longitudinal electron momentum directly at the tunnel exit. The assumption that it is equal to zero is usually adopted [6]. Depending on the phase of the field at the moment when an electron enters the continuum, it then gains a longitudinal momentum while propagating in the laser field, which leads to a final longitudinal momentum distribution.

For the adiabatic limit with Keldysh parameter [1] $\gamma \ll 1$, this acquired longitudinal momentum distribution has width

$$\sigma_{\parallel}^{\mathrm{A}} = \sqrt{\frac{3\omega}{2\gamma^3(1-\epsilon^2)}}, \qquad \gamma = \frac{\omega\sqrt{2I_p}\sqrt{1+\epsilon^2}}{F_0}, \tag{1}$$

with ω denoting the laser frequency, ϵ the ellipticity, I_p the ionization potential and F_0^2 the peak field intensity. On the other hand, the non-adiabatic theory by PPT [3,4] predicts a spread with width

$$\sigma_{\parallel}^{\mathrm{NA}} = \sqrt{\frac{\omega}{2c_x}}, \quad \text{with } c_x = \frac{s_0(1-\epsilon^2)}{(\epsilon - s_0)(1-\epsilon s_0)}\sqrt{\frac{s_0^2+\gamma^2}{1+\gamma^2}}, \quad s_0 \text{ the solution to: } \operatorname{artanh}\left(\sqrt{\frac{s^2+\gamma^2}{1+\gamma^2}}\right) = \frac{\epsilon}{\epsilon-1}\sqrt{\frac{s^2+\gamma^2}{1+\gamma^2}}. \tag{2}$$

It is worth noting that $\sigma_{\parallel}^{\mathrm{NA}} > \sigma_{\parallel}^{\mathrm{A}}$, therefore taking account of non-adiabatic effects leads to a wider momentum spread under the same experimental parameters.

2. Field Intensity Calibration

In strong field experiments, the exact intensity of the laser field must be calibrated based on the measured electron momenta and can not be determined independently to the desired accuracy. The most common and accurate in-situ method is based on the final transverse momentum of electrons freed by an elliptically polarized field [7]. An important non-adiabatic effect is that the likeliest transverse momentum at the tunnel exit is non-zero [4]

$$p_{\perp,\mathrm{initial}}^{\mathrm{NA}} = \frac{\epsilon F_0}{\omega\sqrt{1+\epsilon^2}}\left((1-s_0/\epsilon)\sqrt{\frac{1+\gamma^2}{1-s_0^2}} - 1\right) \neq 0 \text{ au} \tag{3}$$

for $\epsilon \neq 0$, while the adiabatic assumption yields a transverse momentum distribution centered around zero. This leads to larger transverse momentum predictions and consequently to reduced field calibration values for measurements when applying the non-adiabatic momentum-to-intensity mapping [8].

3. Quantitative comparison of Theory and Experiment

The experiment is described in detail elsewhere [9]. The ion momenta during an ellipticity scan of strong field ionization of Helium were recorded in a COLTRIMS setup [10]. The calibrated laser field strengths are given by $F_0^{\mathrm{NA}} = 0.14$ au and $F_0^{\mathrm{A}} = 0.151$ au respectively. The measured longitudinal momentum spreads are considerably wider than the theoretical predictions (Fig. 1), even when the non-adiabatic formula (2) is calculated using the field strength from adiabatic calibration (red dotted). Using non-adiabatic theory [4] to calibrate the field strength compensates for the analytically wider non-adiabatic longitudinal spread, resulting in almost complete agreement in the predictions of both the non-adiabatic (red solid) and adiabatic (blue solid) cases.

In classical trajectory Monte Carlo simulations [9] following adiabatic assumptions, an initial longitudinal momentum spread was varied to find the best fitting value to reproduce the final momentum distribution. Both experimental and simulated momentum distributions were analyzed by elliptical integration [9]. This new method to

analyze angular momentum distribution is robust for any ellipticity and has been successfully applied in studying Coulomb effects for all ranges of polarization [11].

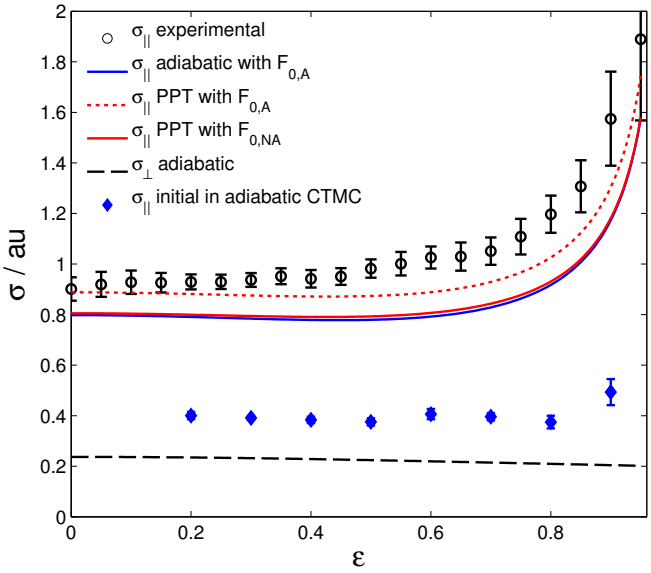

Figure 1. Experimental longitudinal momentum spread **O** [12] compared to theoretical predictions: non-adiabatic spread (2) from adiabatic field strength calibration (red dotted) and from non-adiabatic calibration (red solid) as well as adiabatic spread (1). The best fitting initial momentum spreads ♦ are even larger than the initial transverse momentum (black dashed).

3. Conclusion and Outlook

Our findings show that independent of the uncertainty in the field calibration, current theoretical descriptions can not fully explain the observed longitudinal momentum spread. The initial longitudinal momentum spread that best reproduces the experimental distributions is of the order of twice the transverse momentum spread. Therefore, further theoretical work is necessary to more accurately model the spread of the electron wavepacket in strong field ionization.

References

1. L. V Keldysh, "Ionization in the field of a strong electromagnetic wave," Sov. Phys. JETP **20**, 1307 (1965).
2. N. B. Delone and V. P. Krainov, "Energy and angular electron spectra for the tunnel ionization of atoms by strong low-frequency radiation," J. Opt. Soc. Am. B **8**, 1207–1211 (1991).
3. A. M. Perelomov, V. S. Popov, and M. V. Terent'ev, "Ionization of Atoms in an Alternating Electric Field," Sov. Phys. JETP **23**, 924 (1966).
4. A. M. Perelomov, V. S. Popov, and M. V. Terent'ev, "Ionization of Atoms in an Alternating Electric Field: II," Sov. Phys. JETP **24**, 207–217 (1967).
5. G. L. Yudin and M. Y. Ivanov, "Nonadiabatic tunnel ionization: Looking inside a laser cycle," Phys. Rev. A **64**, 13409 (2001).
6. M. Y. Ivanov, M. Spanner, and O. Smirnova, "Anatomy of strong field ionization," J. Mod. Opt. **52**, 165–184 (2005).
7. A. S. Alnaser, X. M. Tong, T. Osipov, S. Voss, C. M. Maharjan, B. Shan, Z. Chang, and C. L. Cocke, "Laser-peak-intensity calibration using recoil-ion momentum imaging," Phys. Rev. A **70**, 23413 (2004).
8. R. Boge, C. Cirelli, A. S. Landsman, S. Heuser, A. Ludwig, J. Maurer, M. Weger, L. Gallmann, and U. Keller, "Probing non-adiabatic effects in strong-field tunnel ionization," Phys. Rev. Lett. **111**, 103003 (2013).
9. C. Hofmann, A. S. Landsman, C. Cirelli, A. N. Pfeiffer, and U. Keller, "Comparison of different approaches to the longitudinal momentum spread after tunnel ionization," J. Phys. B At. Mol. Opt. Phys. **46**, 125601 (2013).
10. R. Dörner, V. Mergel, O. Jagutzki, L. Spielberger, J. Ullrich, R. Moshammer, and H. Schmidt-Böcking, "Cold Target Recoil Ion Momentum Spectroscopy: a "momentum microscope" to view atomic collision dynamics," Phys. Rep. **330**, 95–192 (2000).
11. A. S. Landsman, C. Hofmann, A. N. Pfeiffer, C. Cirelli, and U. Keller, "Unified Approach to Probing Coulomb Effects in Tunnel Ionization for Any Ellipticity of Laser Light," Phys. Rev. Lett. **111**, 263001 (2013).
12. A. N. Pfeiffer, C. Cirelli, A. S. Landsman, M. Smolarski, D. Dimitrovski, L. B. Madsen, and U. Keller, "Probing the Longitudinal Momentum Spread of the Electron Wave Packet at the Tunnel Exit," Phys. Rev. Lett. **109**, 83002 (2012).